EPJ Web of Conferences **75**, 05006 (2014)
DOI: 10.1051/epjconf/ 201475 05006

Magnetic Properties of $La_{0.8}K_{0.2}MnO_3$ Nanoparticles

M. Mihalik[1a], M. Zentková[1], J.Briančin[2], M. Fitta[3], M.Mihalikjr[1], J. Lazúrová and M. Vavra[1,4],

[1]Institute of Experimental Physics SAS, Watsonova 47, 040 01 Košice, Slovak Republic
[2]Institute of Geotechnics SAS, Watsonova 45, 040 01 Košice, Slovakia
[3]Institute of Nuclear Physics Polish Academy of Sciences, Radzikowskiego 152, 31-342 Kraków, Poland
[4]Institute of Chemistry, Faculty of Science, PJ Šafárik University, Moyzesova 11, 040 01 Košice, Slovakia

Abstract. Magnetic properties of $La_{0.8}K_{0.2}MnO_3$have been studied on nanoparticles prepared by glycine – nitrate method. As prepared nanoparticles and samples annealed at 300°C/2 hours adopt orthorhombic crystal structure (space group *Pbnm*). Crystal structure and particles size were modified by heat treatment. The exchange bias effect was observed on samples with particles size smaller than 50 nm.Cooling in magnetic field $H_{cf} \neq 0$ through the Curie temperature $T_C$shifts hysteresis loop in horizontal and vertical direction. The values of exchange bias field H_E, coercive field H_c, remnant asymmetry μ_E and coercive magnetization μ_c increase with increasing value of cooling field H_{cf}. In addition the training effect was studied. Basic magnetic properties like the Curie temperature T_C and the saturated magnetization $\mu_s$increase and H_E or μ_E decrease with heat treatment. Heat treatment at 600 °C/2 hours increases the average size of nanoparticles to about 60 nm, crystal structure changes to rhombohedral structure (space group $R\bar{3}c$) and EB effect vanishes.

1 Introduction

The exchange bias (EB) was discovered more than 55 years ago, by Meiklejohn and Bean on Co/CoO core–shell nanoparticles [1], and its characteristic signature is the horizontal shift of the centre of magnetic hysteresis loop from its normal position at $H = 0$ to $H_E \neq 0$ and vertical shift which can be characterised by remnant asymmetry μ_E. EB usually occurs in systems which are composed by an antiferromagnet (AFM) that is in atomic contact with a ferromagnet (FM) after the system is cooled, below the respective Néel and Curie temperatures T_N and T_C, in an external cooling field H_{cf}. EB phenomena were observed in various materials like Laves phases, intermetallic compounds and alloys, binary alloys, Heusler alloys [2] or on layered bulk fluorometallo complex [3] where different aspects of magnetism were focused from the EB effect. The first evidence of the EB effect in mixed-valent manganites having perovskite structure was reported in a spontaneously phase separated system $Pr_{1/3}Ca_{2/3}MnO_3$[4] which stimulated new interest for study of the EB effect in structurally single-phase compounds. The EB phenomena attributed to the spontaneous phase separation are very often observed in manganites with different perovskite structures. In the case of a fine particle system the surface to volume ratio becomes significantly large compared to the bulk counterpart. In such a case the surface effect dominates over the core part quite often, leading to a variety of magnetism and core-shell model can provide good interpretation of observed phenomena. Both concepts were frequently used for interpretation of EB effects in the $La_{1-x}Ca_xMnO_3$[5-10], $Nd_{0.5}Ca_{0.5}MnO_3$ [11] and $Pr_{0.5}Ca_{0.5}MnO_3$ [12] nanoparticles. Among manganites, the manganites doped with univalent metals, such as Ag, K, and Na,are of greatest interest, because their physical properties are very sensitive to a magnetic field at room temperature. Group of $La_{1-x}K_xMnO_3$manganites provides a series of new oxides to study magnetocaloric effect [13, 14] and insulator-to-metal transition [15] at room temperature. In our paper we study effect of annealing on magnetic properties of $La_{0.8}K_{0.2}MnO_3$ nanoparticles.

2 Experimental

Preparation of $La_{0.8}K_{0.2}MnO_3$nanopowders followed the glycine-nitrate method, which use glycine as fuel and nitrates as oxidants [16, 17]. Within this procedure, the aqueous solutions of the starting compounds were stirred and heated to dehydrate. Afterwards the solutions became viscous gel which underwent an auto ignition after some

[a] Corresponding author: mihalik@saske.sk

time. After short combustion of only few seconds, black porous ashes of $La_{0.8}K_{0.2}MnO_{3-\delta}$ were formed. A part of as-cast samples were annealed at 300 °C and 600 °C for 2 hours in air atmosphere by a muffle furnace. The oxygen

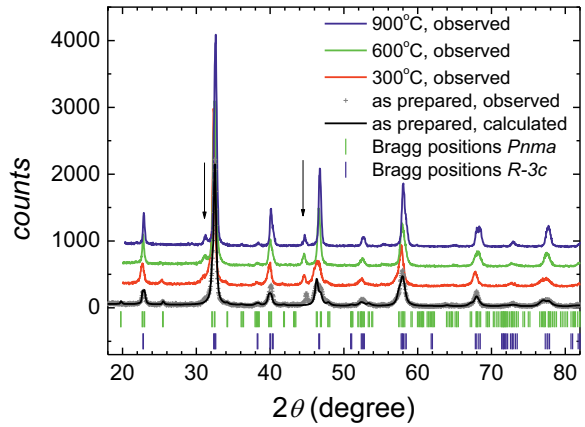

Fig. 1.X-ray powder diffraction patterns for all samples; arrows point to contribution from sample holder.

content (together with mean oxidation state of manganese atoms) in prepared compounds (both as prepared and annealed) was estimated by iodometric titration analysis. The average valence of manganese varies between 3.14 and 3.44. The X-ray powder diffraction (XRD) measurements have been carried out on the X'Pert PRO diffractometer with Cu-K_α radiation (λ_1=1.54056 Å, λ_2=1.54440 Å) and the XRD patterns were identified with the FullProf program [18] based on the Rietveld method [19]. As prepared and annealed samples at 300 °C crystalize in orthorhombic crystal structure (space group *Pnma*) with lattice parameters a = 0.5570(5) nm, b = 0.7773(9)nm, c = 0.5525(1)nm for sample annealed at 300 °C. Crystal structure changes to rhombohedral (space group *R-3c*) with annealing obtaining lattice a = 0.5512(6) nm, c = 1.3385(2)nm for sample annealed at 900 °C. MnO_6 - building blocks of crystal structure aredistorted and tilted. An average size of nanoparticles depends on annealing and varies between30 and 135 nm. Morphology of nanoparticles and their size distribution was studied on powders by scanning electron microscope (SEM) MIRA3 TESCAN. Magnetization and AC susceptibility measurements were performed by a SQUID

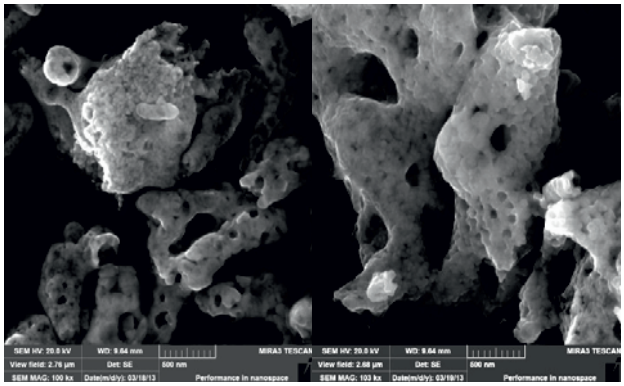

Fig. 2. SEM image for as prepared sample (left) and sample annealed at 900°C/2 hours (right).

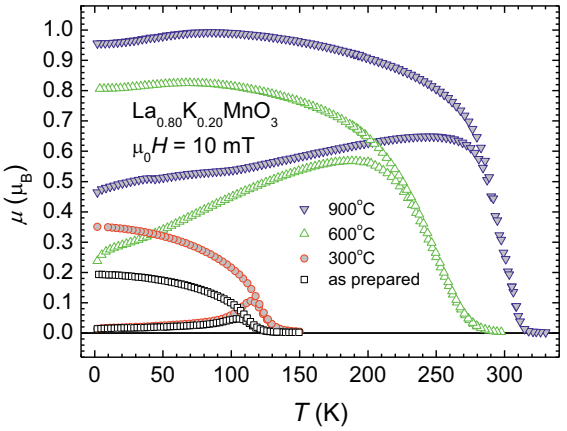

Fig. 3. Magnetization measurements in ZFC and FC regimes are shown for all samples.

magnetometer (MPMS XL−5) in temperature range from 1.8 K to 380 K and in magnetic field up to 5 T.

3 Results and discussion

Our measurements revealed that all samples undergo a paramagnetic (PM) to ferromagnetic (FM) transition at the Curie temperature T_C. The temperature dependences of magnetization in zero field cooled (ZFC) and field cooled (FC) regimes are shown in Fig.3 for all $La_{0.8}K_{0.2}MnO_{3-\delta}$samples. The hysteresis behavior between magnetization measurements performed in ZFC and FC regimes for low applied magnetic fields is typical feature of all samples. Bifurcation temperature T_b is comparable with the Curie temperature T_C. The Curie temperaturewas determined as a minimum on dμ/dT(T) dependence. The increase of ferromagnetic interactions with annealing is evident from all measurements. The Curie temperature increases from T_C = 112.0 K to 295.0 K by annealing. The magnetic susceptibility obeys the Curie Weiss law $\chi = C/(T-\theta)$ for all samples in the

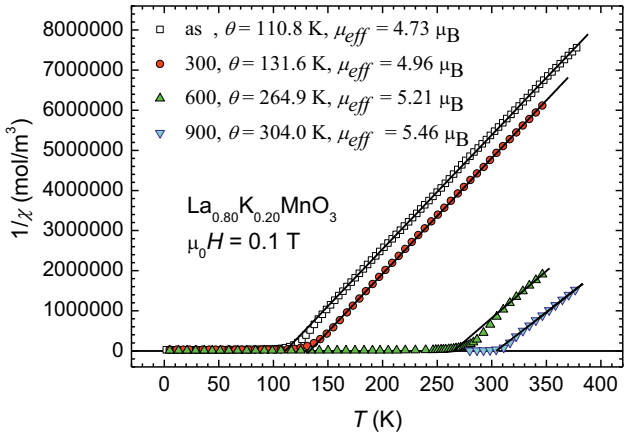

Fig. 4. The inverse susceptibility for all samples, lines represent fits to the Curie Weis law.

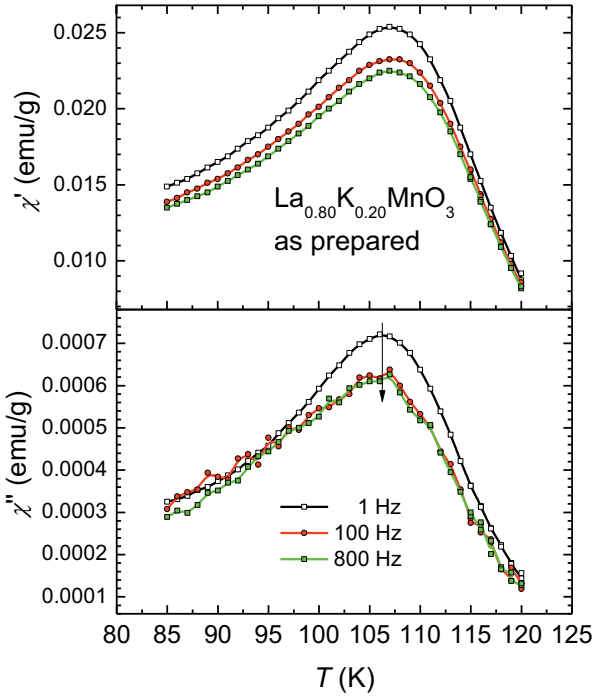

Fig. 5. Sharp peaks in both components of AC susceptibility indicate frequency independent magnetic phase transition.

temperature region high enough above T_C (C is the Curie constant and θ is paramagnetic Curie-Weiss temperature)(Fig.4.). The paramagnetic Curie temperature θ increases with annealing indicating the increase of ferromagnetic interactions in the sample. Simultaneously the effective magnetic moment μ_{eff} increases with annealing. The

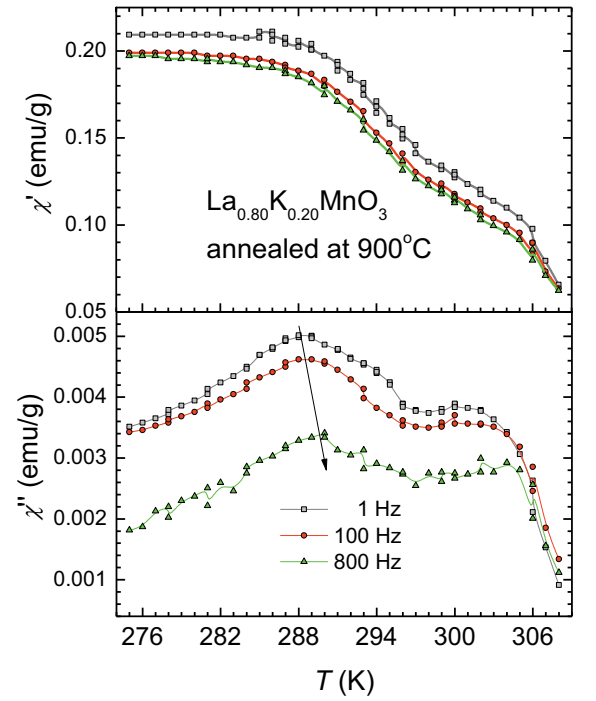

Fig. 6. Two maxima, which are moving to higher temperature with frequency, are observed in both components of AC susceptibility.

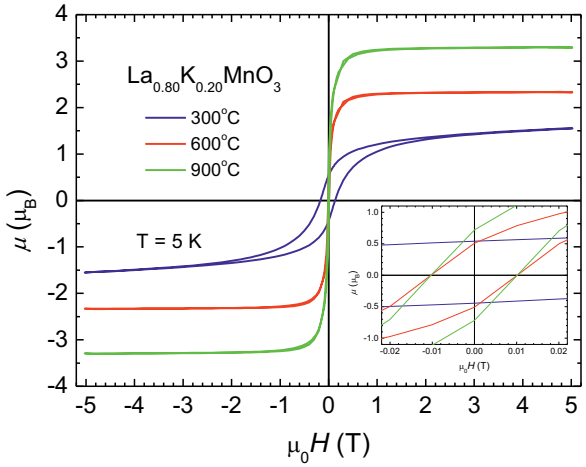

Fig. 7. Ferromagnetic character of hysteresis loops becomes more evident with annealing. The insert shows that hysteresis is typical for all samples.

increase of μ_{eff} cannot be understood assuming oxidation resulting in higher content of Mn^{4+} in samples because the combination of magnetic moments of Mn^{3+} (4.90 μ_B) and Mn^{4+} (3.87 μ_B) in high spin state will result in reduction of μ_{eff}. One possible explanation is that a part of Mn^{3+} in as prepared sample is in low spin state having two unpaired electrons in comparison with high spin state having four unpaired electrons. Annealing will result in the increase of Mn^{3+} in high spin state, which can be connected with gradual change of crystal structure from *Pnma* to $R\bar{3}c$. Evidence for enhanced oxidation was provided by iodometric titration measurements.

The magnetic phase transition is accompanied with an anomaly in both the real part χ' and the imaginary partχ'' of AC susceptibility (Fig.5.), which are frequencydependent in the case of sample annealed at 900°C (Fig.6.). In this case two maxima are seen in the susceptibility at the magnetic phase transition at T_{C1} = 288 K and T_{C2} = 302 K indicating presence of magnetic

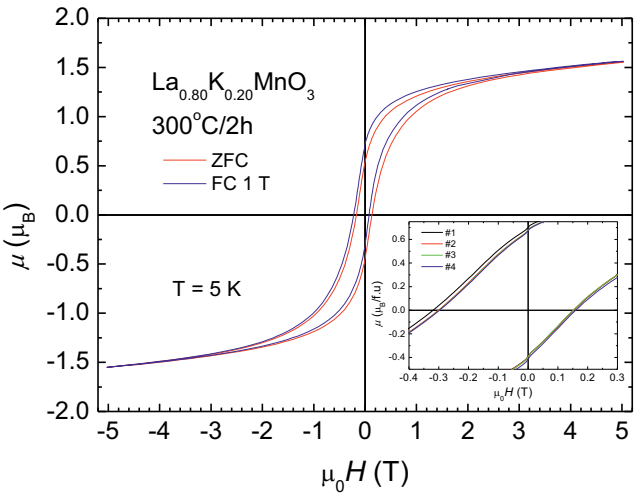

Fig. 8. Ferromagnetic character of hysteresis loops becomes more evident with annealing. The insert shows that hysteresis is typical for all samples.

Inhomogenities in the material. Double transition was observed also in magnetization measurements.

The saturated magnetization μ_s increases with annealing from 1.54μ_B for sample annealed at 300°C to 3.29 μ_B for sample annealed at 900°C (Fig.7). The increase of μ_s can be fully attributed to the increase of ferromagnetic interaction in sample. The remnant magnetization μ_{rem} is increasing and the coercive force H_c is decreasing with annealing (see insert of Fig.7).

The exchange bias effect (EB) was observed on as prepared sample and sample annealed at 300°C (Fig.8.). In these cases the average particle size is less than 50 nm and core shell model can be applied to explain such behaviour. First hysteresis loop (Fig.8.) was measured after cooling down in the zeromagneticfield and before measurement of second loop the sample was exposed to static magnetic field $H_{cf}$and cooled from 150 K through T_C down to 5K. Cooling down in magnetic field $\mu_0 H_{cf}$ = 1 T gives rise to displacement of the magnetic hysteresis loop, which is the typical manifestation of the EB effect. The loop is pinned on vertex in the region of negative magnetization, is tilt and shifted in horizontal and vertical direction. The horizontal shift of the loop is usually expressed by exchange bias field $\mu_0 H_E = \mu_0(H_{c+} - H_{c-})/2$ = 1165 mT; H_{c+} and H_{c-} is coercivefield on positive and negative axes and vertical shift is expressed by the remnant asymmetry $\mu_E = (\mu_{r+} - \mu_{r-})/2 = 0.517\ \mu_B$; μ_{r+} and μ_{r-} is remnant magnetization on positive or negative axis. The difference between subsequent magnetization reversal loops which were measured after cooling in $\mu_0 H_{cf}$ = 1 T, the training effect, is shown in the insert of Fig.8. Measurement of magnetization reversal loop was repeated 4 times at 5 K. Both parameters H_E and μ_E describing the horizontal and vertical shift of loop decrease with consecutive number of cycles and reach stable values.

In conclusion, $La_{0.8}K_{0.2}MnO_3$ nanoparticles have been prepared by glycine – nitrate method with very well developed crystal structure even in as prepared sample. Crystal structure and particles size were modified by heat treatment. As prepared nanoparticles and samples annealed at 300°C/2 hours adopt orthorhombic crystal structure (space group *Pbnm*) and the average particles size is less than 50 nm. Heat treatment at 600 °C/2 hours and at 900 °C/2 increases the average size of nanoparticles from 60 nm to 135 nm, crystal structure changes to rhombohedral structure (space group $R\bar{3}c$). The annealing increases T_C, θ and μ_s mainly due to the enhancement of ferromagnetic exchange interaction given by the double – exchange interaction. The increase of μ_{eff} with annealing we attribute to population of high spin state of Mn^{3+} which can be related to change of crystal structure.EB phenomena were observed on nanoparticles with average size less than50 nm. All parameters describing EB effect have tendency of saturation in relatively low field of about $\mu_0 H_{cf}$ = 0.1 T. The heat treatment at 300°C leads to reduction of coercive force H_c and bias field H_E, on the other hand the coercive magnetization μ_c and remnant asymmetry μ_E increase. Both parameters H_E and μ_E describing the horizontal and vertical shift of loop decrease with consecutive number of cycles in training effect. Heat treatment at 600 °C/2 hours increases the average size of nanoparticles to 60 nm, crystal structure changes to rhombohedral structure (space group $R\bar{3}c$) and EB effect vanishes.Our results suggest that surface effects and core shell model can explain EB phenomena in this case because it is well known that surface effect is important on particle with average size smaller than 50 nm. On the other hand magnetic phase separation in single crystalline phase cannot be completely excluded, too.

Acknowledgement

This work was supported by the projects VEGA2/0178/13, APVV-0132-11 and ERDF EU under the contract No. ITMS26220120005.This work was partiallyfinanced bythe Foundation for Polish Science.

References

1. W. P. Meiklejohn and C. P. Bean, Phys. Rev.**102**, 1413 (1956)
2. S. Giri, M. Patra and S MajumdarJ. Phys.: Condens. Matter **23**, 073201 (2011)
3. Z. Jagličić, M. Zentková, M. Mihalik, Z. Arnold, M. Drofenik, M. Kristl, B. Dojer, M. Kasunič, A. Golobič and M Jagodič, J. Phys.: Condens. Matter **24**, 056002 (2012)
4. D. Niebieskikwiat and M.B. Salamon, *Phys. Rev.* B, **72,** 174422 (2005)
5. X. H. Huang, J. F. Ding, G. Q. Zhang, Y. Hou, Y. P. Yao, and X. G. Li, Phys. Rev B. **78,** 224408 (2008)
6. S.M. Zhou, S.Y. Zhao, L.F. He, Y.Q. Guo, L. Shi, Mat. Chem. and Phys. **120**, 75 (2010)
7. L. Liu, J.J. Zheng, S.L. Yuan, Z.M. Tian, Solid State Communications **150,** 1944 (2010)
8. L. Liu, J.J. Zhenga, Z.C. Xia, S.L. Yuan, Z.M. Tian, Solid State Communications **150**, 2322 (2010)
9. V. Markovich, I. Fita, A. Wisniewski, D. Mogilyansky, R. Puzniak, L. Titelman, C. Martin, and G. Gorodetsky, Phys. Rev. B **81**, 094428 (2010)
10. Xiao H. Huang, Zhen L. Jiang, Xue F. Sun, Xiao G. Li, J. Am. Ceram. Soc., **94,** 1324(2011)
11. L. Liu, S.L. Yuan, Z.M. Tian, X. Liu, J.H. He, P. Li, C.H. Wang, X F Zheng, S Y Yin, J. Phys. D: Appl. Phys. **42,** 045003(2009)
12. T. Zhang and M. Dressel, Phys. Rev. B **80**, 014435 (2009)
13. A.M. Aliev, A.G.Gamzatov, A.B.Batdalov, A.S.Mankevich, I.E.Korsakov, Physica B, **406**, 885 (2011). DOI:10.1016/j.physb.2010.12.021
14. I.K. Kamilov, A.G. Gamzatov, A.B. Batdalov, A.S. Mankevich, and I.E. Korsakov, Bull. Mater. Sci., **32**, 443 (2009).
15. S. B. Bošković, B. Z. Matovic, M. D. Vlajić, V. D. Kristic., Ceram Int **33**, 89 (2007)
16. D. Markovic, V. Kusigerski, M. Tadic, J. Blanusa, M. V. Antisari, V. Spasojevic: *Scr. Mater.***59**, 35 (2008)
17. J. Rodrigues-Carvajal, FullProf.2k Ver. 4.7, ILL., 2010 http://www.ill.eu/sites/fullprof/php/programs.html.
18. M.H. Rietveld Journal of Applied Crystallography, **2**, (1969)